The Correlation Between Cell Structure and Detonation Stability Parameters Across Multiple Fuels and Diluents

David J. Lont and Scott I. Jackson
Department of Aerospace Engineering
Texas A&M University
College Station, TX, USA

1 Introduction

The cell size remains an important experimental parameter in gaseous detonation research because it provides insight into the chemical reaction zone and fluid dynamics driving the wave. Compared to experimental measurements of density or temperature, for example, the cellular structure is readily observable using soot foils or through optical access in narrow channels, such as in [1]. As a result, the detonation cell size has been correlated to various parameters of theoretical and practical importance, such as the critical tube diameter, critical initiation energy, and reaction induction length [2]. Traditionally, only the average is reported in experimental studies and used in analysis, with the extrema or standard deviation sometimes provided (e.g., Ref. [3]). However, more recent studies have proposed that a single length scale is insufficient to characterize detonation cells due to their complex structure [4, 5].

Reactant mixtures are considered irregular if they generate detonation cells with many different sizes and proportions [6]. The activation energy, degree of overdrive, the heat of reaction, and the specific heat ratio have been identified as parameters that control the onset of instability in a detonation [7]. The activation energy has been a well-established parameter as a measure of reactant temperature sensitivity which modulates the cellular structure [7]. The χ stability parameter [8, 9], or alternatively it multiplied by the heat release χQ [10], have also been proposed to characterize irregularity and detonability. All these parameters can be obtained via thermochemical calculation. However, relatively few studies have analyzed the variation in cell size and shape to quantify cellular irregularity from experimental data and have compared them to stability parameters. One such study was that of Ref. [5], who observed a weak correlation between the cell size coefficient of variation and the χ stability parameter for hydrogen mixtures with additives. The present study further investigates the relationship between experimental cellular irregularity and stability parameters by comparing four fuels using soot foils obtained from circular cross-section detonation tubes. The degree of instability is defined in the present study as the apparent irregularity in the cellular structure which can be quantified by some stability parameter.

2 Sources of Experimental Data

The soot foils for ethylene–oxygen–nitrogen mixtures were obtained in a 102-mm inner diameter tube with a length of 3.65 m as discussed in [13]. A soot foil approximately 152 $\times$ 152 mm and 0.3-mm thick made from 430 stainless steel sheet coated with kerosene soot was inserted at the end of the tube and adjacent to the end flange. The mixtures analyzed were at an initial pressure of 1.00 bar and stoichiometric with varying amounts of nitrogen diluent.

Correspondence to: sij@tamu.edu

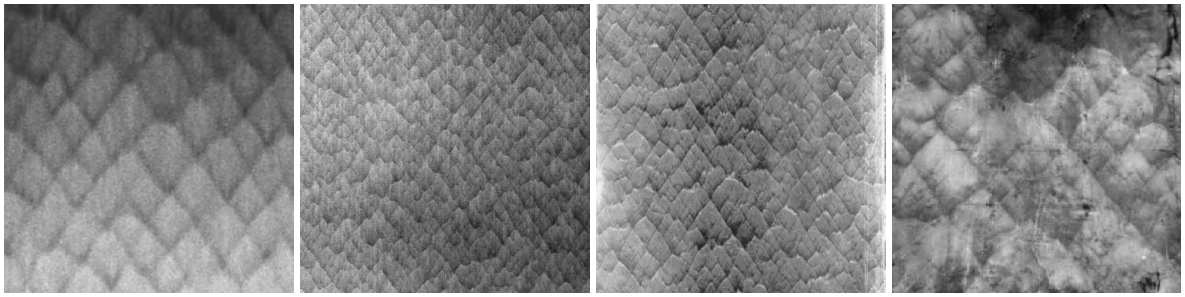

(a) H_2–O_2–80%Ar [3] (b) C_2H_4–O_2–60%N_2 (c) C_3H_8–O_2 [11] (d) 12%CH_4–air [12]

Figure 1: Detonation cellular structure with increasing irregularity. The width of each image is a) 150, b) 100, c) 120, and d) 1,300 mm.

For hydrogen mixtures, two soot foils from Ref. [3] were analyzed: one with 80% argon dilution and another with 60% nitrogen dilution. In the present study, the percentages of diluents are by volume or moles. These were obtained in a 280-mm inner diameter detonation tube at an initial pressure of 0.20 bar. The mixture with argon dilution exhibits a more regular cellular structure compared to the mixture diluted with nitrogen. A stoichiometric propane–oxygen soot foil was obtained from Ref. [11] for an initial pressure of 0.11 bar. For methane, two soot foils from Ref. [12] were analyzed. These had 11 and 12% CH_4 by volume, corresponding to equivalence ratios of 1.18 and 1.30, respectively. They were obtained in a detonation tube that was 520 mm in diameter at an initial pressure of 1.01 bar. Some of the soot foils from these prior studies are shown in Fig. 1. The images are arranged so that the cellular irregularity increases to the right. Additionally, the data from Ref. [5] for the cell size coefficient of variation (ratio of standard deviation to mean) are used for comparison. The coefficient of variation of the cell size quantifies the extent of variability of the individual detonation cells observed with respect to the mean.

3 Methods

Multiple detonation cells were manually traced digitally for each mixture studied. The cell length Λ, width (size) λ, and transverse η_x and axial η_y skews were then obtained for every cell. The transverse skew is defined as the absolute value of the transverse distance between the top and bottom vertices of the detonation cell. Similarly, the axial skew is defined as the axial distance between the left and right vertices of the cell, as illustrated in Fig. 3a. For highly-irregular cells, the extrema are taken to be the vertices. It can be anticipated from inspection from Fig. 1 that mixtures with weak irregularity have low values of skew, while highly-irregular mixtures have high values of skew.

The χ stability parameter was calculated from $\chi = E\Delta_\mathrm{i}/\Delta_\mathrm{e}$ where $E = E_a/(RT_\mathrm{vN})$ is the reduced activation energy. If a global Arrhenius reaction is assumed, the reduced activation energy can be calculated as described in [14] and is given by

$$E = \frac{\mathrm{d}\tau}{\mathrm{d}\left(1/T_\mathrm{vN}\right)} \approx \frac{1}{T_\mathrm{vN}} \left(\frac{\ln \tau_1 - \ln \tau_2}{\frac{1}{T_\mathrm{vN,1}} - \frac{1}{T_\mathrm{vN,2}}} \right) \tag{1}$$

where τ is the induction time from a constant-volume explosion simulation. The states 1 and 2 shown in the subscripts correspond to states with $\pm 1\%$ of the Chapman–Jouguet (CJ) detonation velocity. The nondimensionalized heat release $Q = \Delta h^0/(R_0 T_0)$ was calculated also as described in [14], where the heat of reaction is given by

$$\Delta h^0 = R_\mathrm{CJ} T_\mathrm{CJ} \left(\frac{\gamma_\mathrm{CJ}}{\gamma_\mathrm{CJ} - 1} \right) \left(1 + \frac{\gamma_\mathrm{CJ} - 1}{2} \right) - R_0 T_0 \left(\frac{\gamma_0}{\gamma_0 - 1} \right) \left(1 + \frac{\gamma_0 - 1}{2} M_\mathrm{CJ}^2 \right) \tag{2}$$

The subscripts 0, vN, and CJ respectively correspond to the initial, post shock, and CJ states. The ratio of specific heats was calculated from $\gamma = c^2\rho/P$. The CJ and post-shock states were calculated using SDToolbox [15] and Cantera [16] with the San Diego reaction mechanism [17]. The values for E, χ, Q and γ_{vN} are provided in Table 1 for each mixture analyzed. The equivalence ratio is ϕ and n denotes the number of cells analyzed for each mixture. Because the mean cell aspect ratio for the mixtures studied is roughly constant, only analysis in the transverse direction is presented.

4 Results

Table 1: Gas mixtures and their corresponding parameters for analysis.

Mixture	Diluent	P_0 [bar]	ϕ	E	χ	Q	γ_{vN}	n	Ref.
H_2–O_2	–	0.20	1.00	5.29	13.6	121.1	1.32	–	[5]
H_2–25%Ar	25% Ar	0.20	1.00	4.84	10.9	74.4	1.36	–	[5]
H_2–40%Ar	40% Ar	0.20	1.00	4.39	7.5	77.9	1.40	–	[5]
H_2–50%Ar	50% Ar	0.20	1.00	4.37	7.0	71.3	1.42	–	[5]
H_2–80%Ar	80% Ar	0.20	1.00	4.17	4.7	29.4	1.54	61	[3]
H_2–25%N_2	25% N_2	0.20	1.00	5.31	13.9	19.4	1.32	–	[5]
H_2–40%N_2	40% N_2	0.20	1.00	5.51	16.8	78.5	1.32	–	[5]
H_2–50%N_2	50% N_2	0.20	1.00	5.65	18.1	71.6	1.32	–	[5]
H_2–60%N_2	60% N_2	0.20	1.00	6.46	21.8	57.7	1.32	33	[3]
C_2H_4–O_2	–	1.00	1.00	5.88	16.6	44.6	1.17	102	
C_2H_4–30%N_2	30% N_2	1.00	1.00	6.16	16.3	54.8	1.19	108	
C_2H_4–40%N_2	40% N_2	1.00	1.00	6.42	16.5	57.4	1.21	114	
C_2H_4–50%N_2	50% N_2	1.00	1.00	6.72	15.7	58.8	1.22	105	
C_2H_4–60%N_2	60% N_2	1.00	1.00	7.29	16.2	58.2	1.23	77	
C_2H_4–air	73.82%N_2	1.00	1.00	9.20	17.8	49.4	1.26	30	
C_3H_8–O_2	–	0.11	1.00	10.80	52.9	33.3	1.14	100	[11]
11%CH_4–air	82.72% N_2	1.01	1.18	12.17	1,120.9	39.4	1.25	63	[12]
12%CH_4–air	90.24% N_2	1.01	1.30	12.08	864.4	32.1	1.25	61	[12]

The cell size coefficient of variation σ_λ/λ as functions of E, γ_{vN}, and χ are shown in Fig. 2. The standard deviation is represented by σ. The left and right plots are semilog x-plots, while the center plot is linear. The dashed gray lines in the plots correspond to fits of the data: a logarithmic fit of the form $y = a \log x + b$ where a and b are the fit constants for the semilog plots and the equation of a line for the middle plot. A weak semilogarithmic relationship was observed for E while a weak linear relationship was observed for γ_{vN}. The relationship between the cell size variation and the χ stability parameter is more complex. The best correlation was observed for E, as quantified by the coefficient of determination R^2. This suggests that E and γ_{vN} are better indicators of the experimentally-observed cellular regularity compared to the χ stability parameter. The relationship between the cell size coefficient of variation and the product of χQ was observed to be similar to that with χ alone. If the data for CH_4 are excluded, E and γ_{vN} show stronger correlations.

A similar trend, although with a weaker correlation, can be observed for the skew normalized by the cell size. The transverse skew is normalized by the cell width η_x/λ so that the individual skew of the cells can be directly compared independent of cell size. The coefficient of variation of η_x/λ with varying activation energy is shown in Fig. 3b. As anticipated, mixtures with higher cellular irregularity, quantified by the activation energy, exhibit increased variability in skew. The coefficient of variation of η_x/λ showed the best correlation when plotted as a function of the reduced activation energy, further

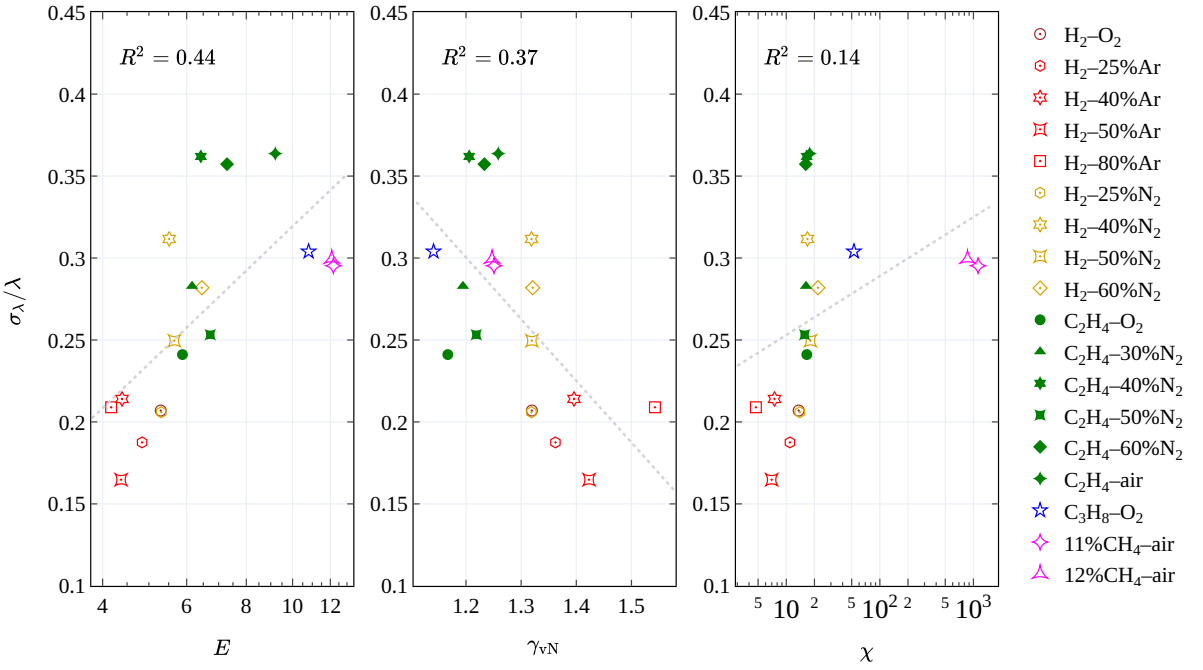

Figure 2: Cell size coefficient of variation for varying activation energy, ratio of specific heats, and χ stability parameter.

suggesting that E is a better quantifier of the experimentally-observed degree of irregularity for the data analyzed.

Histograms for the probability density function (PDF) of the cells sampled for hydrogen, ethylene, propane, and methane mixtures are shown in Fig. 4a. As can be observed from Table 1, H_2–80%Ar corresponds to the lowest value of E while 11%CH_4–air corresponds to the highest value of E for the mixtures studied. Ethylene–oxygen and propane–oxygen mixtures correspond to intermediate values.

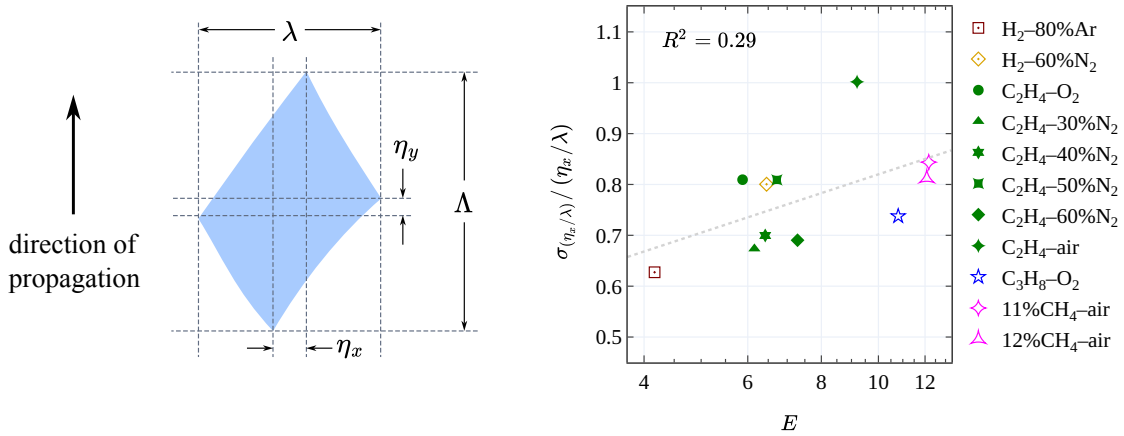

(a) Sketch of detonation cell, showing the width λ, length Λ, and skew η.

(b) Coefficient of variation of the transverse skew normalized by the mean cell size.

Figure 3: Effect of cellular irregularity on cell skew.

The solid curves overlapping the histograms in Fig. 4a show the kernel density estimate (KDE) which estimates the probability density of the dataset while smoothing out noise. The KDE is used instead of the PDF to compare the distributions of these mixtures because the KDE does not require assumptions on the distributions of the cell size data which are not known. As can be observed in Fig. 4a, the distribution of cell sizes is complex and unimodal distributions may not always be appropriate. A focus of future research should be to investigate the distributions of cell sizes for various mixtures.

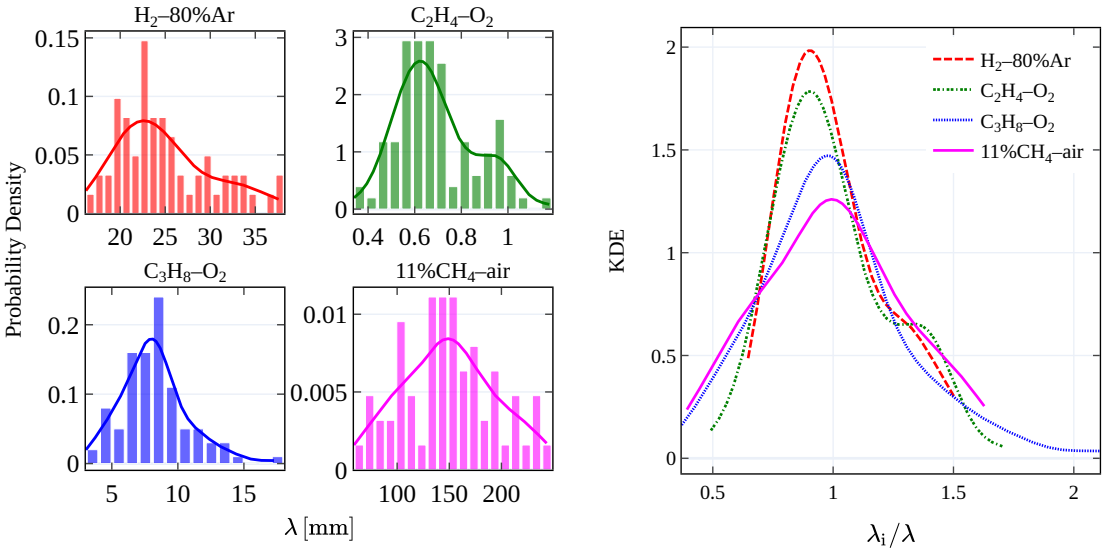

(a) PDF histogram with KDE shown as solid line. (b) KDE as a function of normalized cell size.

Figure 4: Distribution of cell sizes with varying mixture instability.

Direct comparison of the distribution of cell sizes with increasing mixture instability is shown in Fig. 4b. The individual cell sizes λ_i are normalized by the mean cell size λ for each mixture in order to evaluate better the effect of cellular irregularity on the cell size distribution. As anticipated, the mixtures with greater irregularity in their cellular structure exhibit greater variability in cell size while more regular mixtures exhibit less variability in cell size. The mixtures with less irregularity also exhibit right-skewed distributions (Fig. 4a). However, for the mixtures studied, it is not immediately apparent that the skewness in the cell size distribution is correlated to cellular regularity.

5 Summary

The variation of detonation cell size and shape distortion have been experimentally explored as they relate to stability parameters. The coefficient of variation of the cell size appears to be a good experimental quantifier of cell regularity. Although E, γ_{vN}, χ, and χQ have been proposed as thermochemically-derived measures of the degree of cellular irregularity, E and γ_{vN} showed better agreement with the experimentally-observed degree of irregularity. A weaker correlation between skew and reduced activation energy was also observed. It was demonstrated that mixtures with higher degree of instability have a wider distribution of cell sizes. This study further highlights the significance of *cell size distribution* to quantify irregularity and instability, as well as the value of reporting them in addition to the mean cellular scales.

References

[1] M. D. Frederick, R. M. Gejji, J. E. Shepherd, and C. D. Slabaugh. Statistical analysis of detonation wave structure. *Proceedings of the Combustion Institute*, 39(3):2847–2854, 2023. ISSN 1540-7489.

[2] G. Ciccarelli and S. Dorofeev. Flame acceleration and transition to detonation in ducts. *Progress in Energy and Combustion Science*, 34(4):499–550, 2008. ISSN 0360-1285.

[3] F. Pintgen, C. A. Eckett, J. M. Austin, and J. E. Shepherd. Direct observations of reaction zone structure in propagating detonations. *Combustion and Flame*, 133(3):211–229, 2003. ISSN 0010-2180.

[4] V. Monnier, V. Rodriguez, P. Vidal, and R. Zitoun. An analysis of three-dimensional patterns of experimental detonation cells. *Combustion and Flame*, 245:112310, 2022. ISSN 0010-2180.

[5] J. Crane, X. Shi, A. V. Singh, Y. Tao, and H. Wang. Isolating the effect of induction length on detonation structure: hydrogen–oxygen detonation promoted by ozone. *Combustion and Flame*, 200:44–52, 2019. ISSN 0010-2180.

[6] S. T. Kao. *Detonation stability with reversible kinetics*. PhD thesis, California Institute of Technology, 2008.

[7] J. H. S. Lee. *The detonation phenomenon*. Cambridge University Press, New York, 2008.

[8] M. Short and G. J. Sharpe. Pulsating instability of detonations with a two-step chain-branching reaction model: theory and numerics. *Combustion Theory and Modelling*, 7(2):401–416, 2003.

[9] H. D. Ng, M. I. Radulescu, A. J. Higgins, N. Nikiforakis, and J. H. S. Lee. Numerical investigation of the instability for one-dimensional Chapman–Jouguet detonations with chain-branching kinetics. *Combustion Theory and Modelling*, 9(3):385–401, 2005.

[10] M. I. Radulescu, G. J. Sharpe, and D. Bradley. A universal parameter quantifying explosion hazards, detonability and hot spot formation: the χ number. In *ISFEH7 Proceedings of the Seventh International Seminar*, pages 617–626, 2013.

[11] G. J. Sharpe and M. I. Radulescu. Statistical analysis of cellular detonation dynamics from numerical simulations: one-step chemistry. *Combustion Theory and Modelling*, 15(5):691–723, 2011.

[12] M. Kuznetsov, G. Ciccarelli, S. Dorofeev, V. Alekseev, Y. Yankin, and T. H. Kim. DDT in methane-air mixtures. *Shock Waves*, 12(3):215–220, November 2002. ISSN 1432-2153.

[13] D. J. Lont, A. Sethu Venkataraman, A. Padgiotis, M. Martin, E. S. Oran, S. I. Jackson, Y. Huang, and H. A. Farah. Detonation cell size and DDT distance for ethylene-oxygen-nitrogen mixtures. In *AIAA SCITECH 2024 Forum*. American Institute of Aeronautics and Astronautics, 2024.

[14] E. Schultz and J. E. Shepherd. Validation of detailed reaction mechanisms for detonation simulation. Explosion Dynamics Laboratory Report FM99-5, Graduate Aeronautical Laboratories, California Institute of Technology, Pasadena, CA, February 2000.

[15] S. Kao, J. Ziegler, N. Bitter, B. Schmidt, J. Lawson, and J. E. Shepherd. *Shock and Detonation Toolbox*. Pasadena, CA, 2024.

[16] D. G. Goodwin, H. K. Moffat, I. Schoegl, R. L. Speth, and B. W. Weber. Cantera: An object-oriented software toolkit for chemical kinetics, thermodynamics, and transport processes. `https://www.cantera.org`, 2023. Version 3.0.0.

[17] San Diego Mechanism web page. Chemical-kinetic mechanisms for combustion applications. `http://combustion.ucsd.edu`. Mechanical and Aerospace Engineering (Combustion Research), University of California at San Diego.